

Kinetic Analysis of the Role of Histidine Chloramines in Hypochlorous Acid Mediated Protein Oxidation[†]

David I. Pattison* and Michael J. Davies

The Heart Research Institute, 145 Missenden Road, Camperdown, Sydney, NSW 2050, Australia

Received December 2, 2004; Revised Manuscript Received March 20, 2005

ABSTRACT: Hypochlorous acid (HOCl) is a powerful oxidant generated from H₂O₂ and chloride ions by the heme enzyme myeloperoxidase (MPO) released from activated leukocytes. In addition to its potent antibacterial effects, excessive HOCl production can lead to host tissue damage, with this implicated in human diseases such as atherosclerosis, cystic fibrosis, and arthritis. HOCl reacts rapidly with biological materials, with proteins being major targets. Chlorinated amines (chloramines) formed from Lys and His side chains and α -amino groups on proteins are major products of these reactions; these materials are however also oxidants and can undergo further reactions. In this study, the kinetics of reaction of His side-chain chloramines with other protein components have been investigated by UV/visible spectroscopy and stopped flow methods at pH 7.4 and 22 °C, using the chloramines of the model compound 4-imidazoleacetic acid and *N*- α -acetyl-histidine. The second-order rate constants decrease in a similar order (Cys > Met > disulfide bonds > Trp \sim α -amino > Lys \gg Tyr > backbone amides > Arg) to the corresponding reactions of HOCl, but are typically 5–25 times slower. These rate constants are consistent with His side-chain chloramines being important secondary oxidants in HOCl-mediated damage. These studies suggest that formation and subsequent reactions of His side-chain chloramines may be responsible for the targeted secondary modification of selected protein residues by HOCl that has previously been observed experimentally and highlight the importance of chloramine structure on their subsequent reactivity.

Hypochlorous acid (HOCl) is a strong oxidant that plays an important role in the human immune system (1), and is also used extensively as a disinfection agent (bleach) both industrially and domestically (2). In vivo, it is generated by the heme enzyme myeloperoxidase (MPO)¹, which is released into phagosomal vacuoles or the extracellular space by activated phagocytes (neutrophils, monocytes, and possibly macrophages). MPO catalyzes the oxidation of chloride ions by hydrogen peroxide to yield HOCl (1, 3). In addition to its potent antibacterial properties, HOCl-mediated oxidation of host tissues has been observed in numerous diseases (e.g., atherosclerosis, cystic fibrosis, sepsis, kidney disease, and some cancers), with this damage linked to these pathologies (4–9).

HOCl reacts rapidly with a wide variety of biological materials (reviewed in ref 10, 11), but due to the high abundance of amino acids, peptides, and proteins in extracellular fluid, these are likely to be the major targets. The most reactive sites on proteins with HOCl are the sulfur-containing amino acid side chains of Met and Cys (both $k > 10^7 \text{ M}^{-1} \text{ s}^{-1}$) and cystine ($k \sim 10^5 \text{ M}^{-1} \text{ s}^{-1}$) (12–15). These reactions give rise to Met sulfoxide from Met, and

disulfides and oxy acids from Cys and cystine (reviewed in ref 10)); none of these products retain any of the oxidizing ability of HOCl. The amine functions of His ($k \sim 10^5 \text{ M}^{-1} \text{ s}^{-1}$) and Lys ($k \sim 5 \times 10^3 \text{ M}^{-1} \text{ s}^{-1}$) side chains, together with α -amino groups ($k \sim 10^5 \text{ M}^{-1} \text{ s}^{-1}$), are also kinetically favored sites of reaction with HOCl on proteins (2, 12, 13), with these reactions giving rise to chloramines (RNHCl, RR'NCl) and, at higher HOCl concentrations, dichloramines (RNC₂) (10, 11, 16). Unlike the products from the sulfur-containing residues, chloramines retain the oxidizing capacity of HOCl and can undergo secondary reactions, although they are typically milder, more selective oxidants (16–21).

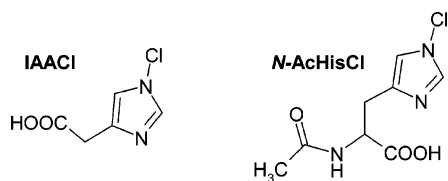
In the absence of other substrates, chloramines undergo slow hydrolysis to yield aldehydes and ketones (22), or in the presence of one electron reductants such as metal ions or superoxide radicals, yield nitrogen-centered radicals (23–25). Chloramines can also transfer chlorine to other substrates, resulting in regeneration of the parent amine and secondary damage to other targets (17–21). Thus, it has been proposed that formation of 3-chloro-Tyr (Cl-Tyr; a specific marker for HOCl-mediated protein oxidation) in vivo can occur via both direct HOCl attack and via transfer from chloramines (26). This is consistent with kinetic data that show the Tyr side chain is a poor direct target for HOCl ($k \sim 50 \text{ M}^{-1} \text{ s}^{-1}$) compared to other protein sites (13). Chlorine transfer from Lys chloramine to Tyr in a -Tyr-X-X-Lys- motif (where X is an amino acid that is unreactive with HOCl) has recently been postulated as a mechanism for regiospecific Tyr chlorination in high-density lipoproteins (HDL) (27).

[†] This work was funded by grants from the Australian Research Council and the National Health and Medical Research Council.

* To whom correspondence should be addressed: Telephone: +61-2-9550-3560. Fax: +61-2-9550-3302. E-mail: d.pattison@hri.org.au.

¹ Abbreviations: apo A-I, apolipoprotein A-I; Cl-Tyr, 3-chlorotyrosine; Cl₂-Tyr, 3,5-dichlorotyrosine; GSH, reduced glutathione; HDL, high-density lipoprotein; HPLC, high-performance liquid chromatography; MPO, myeloperoxidase; *N*-Ac-Cl-Tyr, *N*- α -acetyl-3-chlorotyrosine; *N*-Ac-Cl₂-Tyr, *N*- α -acetyl-3,5-dichlorotyrosine; TNB, 5-thio-2-nitrobenzoic acid.

Chart 1: Chemical Structures of the Chloramines of 4-imidazoleacetic Acid (IAACl) and *N*- α -acetyl-His (*N*-AcHisCl) Used for the Kinetic Studies



There is a growing body of evidence consistent with chloramines being key mediators of cellular damage, including inhibition of DNA repair (28), modulation of apoptotic pathways (29), inactivation of intracellular enzymes (30), and cell death (21, 30). It is likely that these effects arise, at least in part, from secondary chlorine transfer reactions of chloramines. As chloramines are less reactive and more selective than HOCl, they can diffuse considerable distances, including through cell membranes, resulting in oxidative damage to molecules remote from the initial site of HOCl production (19, 21).

Despite the potential importance of chloramines as key intermediates in HOCl-mediated cellular damage, relatively little is known about the kinetics and products of their chlorine transfer reactions. The rate constants for reactions of taurine, Gly, and histamine chloramines with thiols have been reported to be slower than for HOCl itself and are faster with more acidic thiols (20, 21); this may have important implications in determining which thiols are oxidized *in vivo*. Reactions of *cyclo*-(Gly)₂ chloramide are typically 10³–10⁶ times slower than the corresponding reactions of HOCl (31). The reactivity of chloramines formed on pyrimidine bases has also been studied (31). Those formed on the heterocyclic R₂NH positions of thymidine and uridine derivatives oxidize substrates with rates only 10–100 times slower than HOCl (18, 31), whereas chloramines formed on the exocyclic RNH₂ positions of cytidine derivatives react with GSH at rates ca. 10⁴ times slower than HOCl (18). Experimental and computational data have been presented for His and Lys side-chain chloramines being major products of initial HOCl attack on proteins (13, 32), but limited data are available on the kinetics of their chlorine transfer reactions. As the imidazole ring of the His side chain is related to the heterocyclic bases of thymidine and uridine chloramines, chloramines formed on the His side chain might also be expected to undergo rapid chlorine transfer reactions.

In the current work, the second-order rate constants for the reactions of His side-chain (imidazole) chloramines with other protein targets have been determined using the chloramines of 4-imidazoleacetic acid and *N*- α -acetyl-His (see Chart 1). HPLC techniques have also been used to investigate the ability of a range of chloramines/amides that may be generated on proteins to chlorinate *N*- α -acetyl-Tyr. The data obtained suggest that His side-chain chloramines are key intermediates in HOCl-mediated protein damage, as they can rapidly oxidize further substrates. In light of these data, it is postulated that His side-chain chloramines may be responsible for the targeted modification of selected protein residues by HOCl (cf. data in ref 27). The results also highlight the importance of chloramine structure on their subsequent reactivity, as the extent of secondary chlorination

induced by chloramines/amides is observed to vary dramatically.

EXPERIMENTAL PROCEDURES

Materials. All chemicals were obtained from Sigma/Aldrich/Fluka (Castle Hill, NSW, Australia), and used as received, with the exception of sodium hypochlorite (in 0.1 M NaOH, low in bromine, BDH Chemicals, Poole, U.K.) and *N*- α -acetyl-Met-OMe (Bachem, Bubendorf, Switzerland). The HOCl was standardized by measuring the absorbance at 292 nm at pH 12 ($\epsilon_{292}(\text{OCl}^-) = 350 \text{ M}^{-1} \text{ cm}^{-1}$ (33)). All studies (unless otherwise stated) were performed in 0.1 M phosphate buffer (pH 7.4) which was prepared using Milli Q-treated water and treated with Chelex resin (BioRad, Hercules, CA) to remove contaminating transition metal ions. The pH values of solutions were adjusted, where necessary, to pH 7.4 using 100 mM H₂SO₄ or 100 mM NaOH.

Preparation of Chloramines. For stopped flow studies, 4-imidazoleacetic acid and *N*- α -acetyl-His chloramines were prepared by mixing HOCl (10 mM in phosphate buffer) with either 4-imidazoleacetic acid or *N*- α -acetyl-His (11 mM in phosphate buffer) in equal volumes. The reaction was left for ca. 1 min before further dilution with phosphate buffer to the required concentration of chloramine (typically 23 μM to 2.3 mM as determined by reaction with 5-thio-2-nitrobenzoic acid (TNB) (16, 24)). Fresh solutions of the imidazole chloramines were prepared for each kinetic run and used within 30–60 min of preparation. Under the described conditions (at 22 °C), no significant decay of 4-imidazoleacetic acid chloramine (400–450 μM) was detected over 90 min ($p > 0.05$), whereas with *N*- α -acetyl-His chloramine, significant decomposition (to ~90% of the initial concentration) was observed after only 60 min ($p < 0.05$). These data are in contrast to a previous report that suggests the products generated upon treatment of *N*- α -acetyl-His with HOCl do not display any reactivity with TNB, although neither the ratio of reactants nor the time after mixing was reported (21).

For the HPLC studies on chlorination of *N*- α -acetyl-Tyr, the chloramines of 4-imidazoleacetic acid, *N*- α -acetyl-His, ϵ -amino-*n*-caproic acid (a Lys side-chain chloramine model), and Gly (an α -amino chloramine), and the chloramide of *cyclo*-(Gly)₂ (a backbone chloramide model) were prepared by mixing 1.0 mM HOCl with a 2.0 mM solution of the parent amine (both in 0.1 M phosphate buffer, pH 7.4) in equal volumes. The resulting solutions were left for 2 min to allow complete conversion to the corresponding chloramine/amide, before dilution into *N*- α -acetyl-Tyr-containing solutions.

Stopped Flow Studies. The apparatus and procedures used for the stopped flow studies have been described in detail previously (13, 34). In brief, either an Applied Photophysics SX.18MV system (10 ms to 10 s time scale) or a Perkin-Elmer Lambda 40 UV/vis spectrometer with a Hi-Tech SFA 20 attachment (5 s to 15 min time scale) was used. Both systems had a 10 mm path length and were maintained at either 10 or 22 °C by circulating water from a thermostated water bath.

Kinetic data were accumulated at 10 nm intervals between 230 and 350 nm (0.1 M phosphate buffer baseline) and combined to give time-dependent spectral data. In all

experiments, the chloramines were the limiting reagent, with at least a 2-fold excess of substrate (typically 23 μM to 2.5 mM chloramine, 0.1–25 mM substrate). This limits the occurrence of secondary reactions and, at higher substrate excesses, reduces the kinetics to pseudo-first-order which facilitates analysis. Data were processed by global analysis methods, using Specfit software (version 3.0.36, Spectrum Software Associates, USA; see <http://www.bio-logic.fr/rapid-kinetics/specfit.html> for further details). All second-order rate constants reported are averages of at least six determinations, and errors are specified as 95% confidence limits.

UV/Vis Spectroscopy. UV/vis spectroscopy was undertaken on a Perkin-Elmer Lambda 40 spectrometer. Spectra were typically acquired (relative to a 0.1 M phosphate buffer baseline) between 220 and 320 nm ($\Delta\lambda$, 2 nm) with a scan rate of 960 nm min^{-1} and a time interval of 45 s to 30 min depending on the reaction time scale. Temperature control (22 °C) was achieved with a Peltier block. Data were imported into Specfit software, and the kinetics processed by global analysis techniques (as above).

HPLC Instrumentation and Methods. Analysis and quantification of *N*- α -acetyl-Tyr, *N*- α -acetyl-3-chlorotyrosine (*N*-Ac-Cl-Tyr), and *N*- α -acetyl-3,5-dichlorotyrosine (*N*-Ac-Cl₂-Tyr) was carried out on a Shimadzu LC-10A HPLC system (Shimadzu, South Rydalmere, NSW, Australia). The reaction mixtures were separated on a Zorbax reverse-phase HPLC column (25 cm \times 4.6 mm, 5 μm particle size, Agilent Technologies, North Ryde, NSW, Australia) packed with octadecylsilanized silica, equipped with a Pelliguard guard column (2 cm, Supelco, Castle Hill, NSW, Australia). The column was maintained at 30 °C using a column oven (Waters Corporation, Milford, MA). The mobile phase comprised of a gradient of solvent A (10 mM phosphoric acid with 100 mM sodium perchlorate at pH 2.0) and solvent B (80% (v/v) methanol in Nanopure H₂O) eluting at 1 mL min^{-1} . The gradient was programmed as follows: 0–5 min, elution with 80% solvent A and 20% solvent B; over the next 5 min, the proportion of solvent B was increased to 40%; isocratic elution at 40% solvent B occurred for 15 min; over the following 1 min, solvent B was increased to 50% and the column was washed at 50% solvent B for 4 min; over the subsequent 5 min, the proportion of solvent B was reduced to 20% and the column was allowed to re-equilibrate for 5 min prior to injection of the next sample. The eluent was monitored in series by a UV detector (280 nm) and a single channel electrochemical detector (Intro, Antec Leyden) set to an oxidation potential of +1.2 V. Peak areas were determined using Class VP 6.0 software (Shimadzu) and compared to authentic standards. When these conditions were used, *N*- α -acetyl-Tyr was detected in the UV trace at a retention time of 10.3 min, *N*-Ac-Cl-Tyr at 15.8 min, and *N*-Ac-Cl₂-Tyr at 21.8 min; elution times with electrochemical detection were \sim 0.1 min later.

The *N*-Ac-Cl-Tyr and *N*-Ac-Cl₂-Tyr standards were prepared by reacting *N*- α -acetyl-Tyr (2.5 mM) with an excess of HOCl (3.75 mM) in acetate buffer (5 mM, pH 5.4) for at least 1 h (22 °C). The products were separated on a Shimadzu LC-10A HPLC system fitted with a UV detector (280 nm) and an automated fraction collector (FRC-10A; Shimadzu), using a Zorbax SB-C18 semipreparative column (25 cm \times 9.4 mm, 5 μm particle size, Agilent) equipped with a

preparative SB-C8 guard column (1.5 cm \times 9.4 mm, 7 μm particle size, Agilent). The column was maintained at 30 °C using a column oven (Waters Corporation, Milford, MA). The products were eluted isocratically with 32% (v/v) methanol in Nanopure H₂O containing 0.06% trifluoroacetic acid at a flow rate of 3 mL min^{-1} . The *N*-Ac-Cl-Tyr (retention time, 13.9 min) and *N*-Ac-Cl₂-Tyr (retention time, 27.3 min) peaks were collected, and fractions from a series of injections were pooled together prior to reducing the volume to 1–2 mL overnight in a Speedvac concentrator (Savant, Farmingdale, NY). The concentrations of the resulting solutions were quantified by the UV absorbance at $\lambda_{\text{max}} \sim$ 280 nm using published extinction coefficients for nonacetylated Cl-Tyr and Cl₂-Tyr (35).

Statistical Analysis. Statistical analyses of the stabilities of 4-imidazoleacetic acid and *N*- α -acetyl-His chloramines were carried out using 1-way ANOVA with Dunnett's post hoc test. Statistical analyses to compare the HPLC results from the UV and electrochemical detectors, and to examine the effect of time on the extent of chlorine incorporation by the various chlorinating agents, were performed using 2-way ANOVA with Bonferroni post hoc testing. Statistical analysis of the chlorine transfer efficiency of the different chlorinating agents at fixed time points (1 h or 9 days) were analyzed using 1-way ANOVA with Tukey's post hoc test. All statistical analyses were performed using GraphPad Prism 4 (GraphPad Software, San Diego, CA).

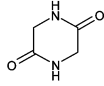
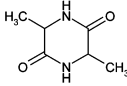
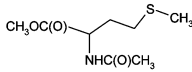
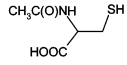
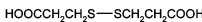
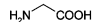

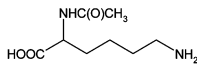
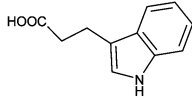
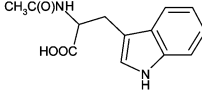
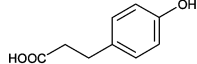
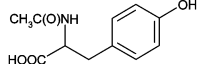
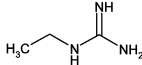
RESULTS

Kinetics of His Side-Chain Chloramine Reactions with Backbone Amide Groups. The abundance of peptide (backbone amide) bonds in proteins relative to any particular side chain makes them a potential target for secondary oxidation by reactive chloramines. Reaction at such sites has been implicated in protein fragmentation, so that damage at these functions may be functionally significant (24). Previous studies show that cyclic dipeptides (e.g., *cyclo*-(Gly)₂) are particularly reactive with HOCl (13); thus, these compounds are good models for estimating the maximal extent of backbone damage that is likely to be induced by this oxidant.

The reactions of 4-imidazoleacetic acid chloramine (1.0 mM) with *cyclo*-(Gly)₂ and *cyclo*-(Ala)₂ (both 5.0–11.0 mM) were sufficiently slow at 22 °C (time scales of 6 and 10 min for *cyclo*-(Gly)₂ and *cyclo*-(Ala)₂, respectively) that UV/vis scans could be used to monitor the reaction following mixture of the reactants with the SFA20 stopped flow accessory. The 4-imidazoleacetic acid chloramine absorbance was observed to decay over the full spectral range ($\lambda = 240$ –320 nm), indicating significant reaction with these substrates. At shorter wavelengths ($\lambda < 260$ nm) a further increase in absorbance was detected at longer times, presumably due to subsequent reactions of the chloramides formed (as seen with HOCl (13, 31)). Data analysis (4-imidazoleacetic acid chloramine + amide \rightarrow 4-imidazoleacetic acid + chloramide) was undertaken at $\lambda > 260$ nm, as this allowed a clean decay of the 4-imidazoleacetic acid chloramine to be measured without the confounding influence of other absorbing products. The resulting second-order rate constants (per amide group) for these reactions are given in Table 1.

The reactivity of 4-imidazoleacetic acid chloramine (1.0 mM) with *N*- α -acetyl-Ala (25.6 mM) was also investigated

Table 1: Second-Order Rate Constants (with 95% Confidence Limits) at 22 °C (Unless Otherwise Stated) and pH 7.2–7.5 (0.1 M Phosphate Buffer) for the Reactions of 4-imidazoleacetic Acid (IAACl) or *N*- α -acetyl-His (*N*-AcHisCl) Chloramines with Amino Acid Side Chains, Free α -Amino Groups, and Backbone Amides

Substrate	Structure	k_2 (IAACl) / $\text{M}^{-1} \text{s}^{-1}$	k_2 (<i>N</i> -AcHisCl) / $\text{M}^{-1} \text{s}^{-1}$
Cyclo-(Gly) ₂		3.2 ± 0.4^a	ND
Cyclo-(Ala) ₂		1.4 ± 0.2^a	ND
<i>N</i> - α -acetyl-Met-OMe		$(1.3 \pm 0.1) \times 10^6^b$	$(6.9 \pm 0.4) \times 10^5^b$
<i>N</i> - α -acetyl-Cys		$> 5 \times 10^6^c$	ND
3,3'-dithiodipropionic acid		$(2.10 \pm 0.02) \times 10^4$	$(1.9 \pm 0.1) \times 10^4$
Gly		$(1.77 \pm 0.05) \times 10^3$	ND
ϵ -amino- <i>n</i> -caproic acid		210 ± 40	ND
<i>N</i> - α -acetyl-Lys		210 ± 20	ND
3-indolepropionic acid		$(2.6 \pm 0.3) \times 10^3$	$(2.8 \pm 0.2) \times 10^3$
<i>N</i> - α -acetyl-Trp		$(1.7 \pm 0.2) \times 10^3$	ND
3-(4-hydroxyphenyl)propionic acid		5.5 ± 0.8	7 ± 1
<i>N</i> - α -acetyl-Tyr		7.2 ± 0.7	9 ± 2
Ethyl guanidine		1.3 ± 0.1	ND

^a The second-order rate constants are expressed per amide group; therefore, the second-order rates for the substrate are double these values.

^b Rate constant measured at 10 °C, as the absorbance changes were within the dead time (~2.5 ms) of the apparatus at 22 °C. ^c Reaction too fast to obtain accurate kinetic data, even at 10 °C. ND, rate not determined.

to eliminate possible effects of the cyclic structure on these reactions, and to ensure that the *N*- α -acetyl group employed in subsequent studies was not a major competing target for chlorine transfer. The spectral changes observed in both the presence and absence of *N*- α -acetyl-Ala were identical over a period of 18 h, indicating that chlorine transfer to *N*- α -acetyl-Ala did not compete with the decomposition of 4-imidazoleacetic acid chloramine.

Rate Constants for the Quenching of His Side-Chain Chloramines by Sulfur-Containing Amino Acid Side Chains. Cys, Met, and cystine are known to be kinetically preferred targets for HOCl and many chloramines (12, 13, 15, 18, 20, 21, 31, 36). The absorbance changes that occurred on reaction of 4-imidazoleacetic acid or *N*- α -acetyl-His chloramines (both 250 μM) with *N*- α -acetyl-Met-OMe (300–730 μM) were too fast to measure directly at 22 °C. When the

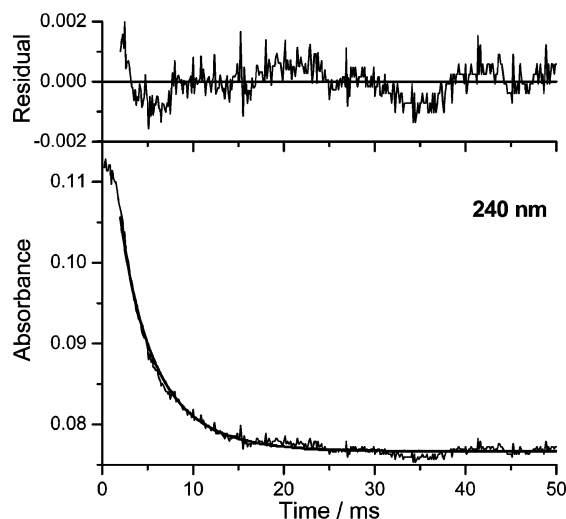


FIGURE 1: Graph showing the change in absorbance at 240 nm (over 50 ms) for the reaction of *N*- α -acetyl-His chloramine (250 μ M) with *N*- α -acetyl-Met-OMe (550 μ M) at 10 $^{\circ}$ C. In the main graph, the experimental data are shown together with the fit obtained from global analysis for $t > 2$ ms (to avoid interference from the apparatus dead time). The residual absorbance between the experimental data and the corresponding fit is shown above the main panel.

temperature was reduced to 10 $^{\circ}$ C, small absorbance decreases ($\Delta A < 0.05$) were detected across the spectral region from 230 to 300 nm ($t < 50$ ms), consistent with chloramine consumption. Despite the low-molar excess of *N*- α -acetyl-Met-OMe over chloramines, the data were fitted well with a second-order mechanism (imidazole chloramine + *N*- α -acetyl-Met-OMe \rightarrow imidazole + *N*- α -acetyl-Met-OMe product) that was first order in both the imidazole chloramine and *N*- α -acetyl-Met-OMe. The data were fitted by global analysis from $t > 2$ ms to prevent interference from the apparatus dead time; a sample fit at 240 nm together with the residual absorbance between the fit and experimental data is shown (Figure 1). These analyses yielded the second-order rate constants given in Table 1. The absorbance changes observed under identical conditions with *N*- α -acetyl-Cys were distorted by the dead time of the apparatus, precluding accurate determination of the second-order rate constant for this process. However, the data did allow a lower limit for the reaction to be estimated at 10 $^{\circ}$ C (Table 1), assuming an analogous mechanism to that given above for *N*- α -acetyl-Met-OMe.

Reactions of 4-imidazoleacetic acid and *N*- α -acetyl-His chloramines with the cystine model compound, 3,3'-dithiodipropionic acid were markedly slower than for the above Cys and Met models, allowing the reactions to be monitored directly at 22 $^{\circ}$ C. With both imidazole chloramines (250 μ M), increases in absorbance ($\Delta A \sim 0.1$) were detected ($t = 200$ –500 ms) from 230 to 260 nm, with concomitant small absorbance decreases at longer λ , on reaction with 3,3'-dithiodipropionic acid (950 μ M to 2.7 mM). These changes were readily fitted to a simple second-order mechanism (e.g., *N*- α -acetyl-His chloramine + 3,3'-dithiodipropionic acid \rightarrow *N*- α -acetyl-His + product) to give second-order rate constants (Table 1).

Kinetics of His Side-Chain Chloramine Reactions with Amines: α -Amino Groups and Lys Side Chains. Amine groups are known to be important kinetic targets on proteins

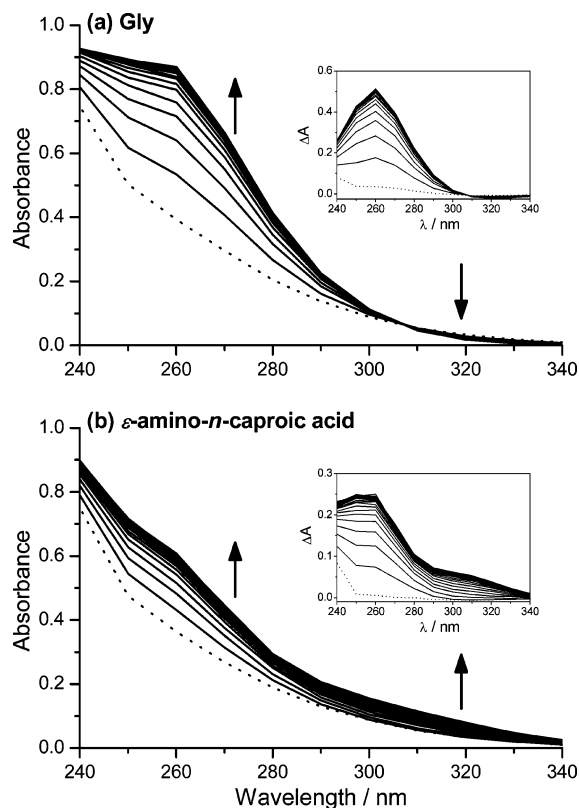


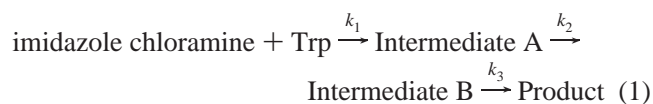
FIGURE 2: Graph showing the time-dependent spectral changes upon reaction of 4-imidazoleacetic acid chloramine (2.5 mM) with (a) an α -amino group, Gly (24.0 mM) and (b) a Lys side-chain model, ϵ -amino-*n*-caproic acid (17.2 mM). In both graphs, the dotted spectrum corresponds to that obtained 2 ms after mixing 4-imidazoleacetic acid chloramine with the respective amines; further spectra are given in (a) at 10 ms intervals to a final time of 200 ms and in (b) at 100 ms intervals to a final time of 5 s. The arrows show the direction of absorbance change in each spectral region. In both (a) and (b), the inset figures show the absorbance changes with the baseline absorbance for 4-imidazoleacetic acid chloramine subtracted, highlighting that only monochloramines (λ_{\max} , 260 nm) are formed with Gly (a) but both mono- (λ_{\max} , 250 nm) and di- (λ_{\max} , 300 nm) chloramines are generated with ϵ -amino-*n*-caproic acid (b).

for HOCl due to their reactivity and abundance. Therefore, reaction of 4-imidazoleacetic acid chloramine (2.5 mM) with Gly (8.0–24.7 mM) was examined at 22 $^{\circ}$ C over a period of 0.5–1 s, to ascertain the second-order rate constant for transfer to α -amino groups. Over time, an increase in absorbance was detected at $\lambda < 300$ nm, and a small loss in absorbance was observed at longer wavelengths (Figure 2a). Subtraction of the 4-imidazoleacetic acid chloramine absorbance from the data revealed the growth of a band with $\lambda_{\max} = 260$ nm (Figure 2a, inset), consistent with the formation of Gly monochloramine (13). The data were fitted well with a simple mechanism (4-imidazoleacetic acid chloramine + Gly \rightarrow 4-imidazoleacetic acid + Gly monochloramine) to give the second-order rate constant in Table 1.

The rates of chlorine transfer from 4-imidazoleacetic acid chloramine (2.5 mM) to ϵ -amino-*n*-caproic acid and *N*- α -acetyl-Lys (both between 8.6 and 25.8 mM) were investigated as models of the Lys side chain. For both substrates, an increase in absorbance was observed over a time scale of 2–5 s, between 240 and 340 nm (Figure 2b). Following subtraction of the 4-imidazoleacetic acid chloramine absorbance from the data, two absorbance peaks were detected

with $\lambda_{\max} = 250$ and 300 nm (Figure 2b, inset). The extent of formation of the peak at 300 nm was greatest at low-molar excesses of ϵ -amino-*n*-caproic acid or *N*- α -acetyl-Lys over 4-imidazoleacetic acid chloramine, and the kinetics monitored at 310 nm showed a lag phase of a few hundred ms (data not shown) relative to the data at shorter wavelengths (e.g., 250 nm), where the absorbance increased immediately after the dead time (<2.5 ms) of the apparatus. These data are consistent with the formation of the monochloramines of ϵ -amino-*n*-caproic acid or *N*- α -acetyl-Lys at 250 nm and subsequent secondary chlorination to form the corresponding dichloramines ($\lambda_{\max} \sim 310$ nm). To obtain accurate kinetic data, only conditions that favored monochloramine formation were analyzed; thus, only wavelengths < 280 nm, from experiments with ≥ 6 -fold excess of amine, were used for analysis. When these criteria were used, it was possible to fit the data to a simple mechanism (4-imidazoleacetic acid chloramine + amine \rightarrow 4-imidazoleacetic acid + monochloramine) yielding the second-order rate constants listed in Table 1. Reliable estimates of the rate constants for secondary chlorination of the monochloramines could not be obtained from these data.

Kinetics of His Side-Chain Chloramine Reactions with the Trp Side Chain. Reaction of the Trp side chain with 4-imidazoleacetic acid chloramine was studied at 22 °C using 3-indolepropionic acid and *N*- α -acetyl-Trp as substrates. Stopped flow studies of 4-imidazoleacetic acid chloramine (25 μ M) with 3-indolepropionic acid or *N*- α -acetyl-Trp (80–160 μ M) over 4–5 min yielded complex absorbance changes as observed with HOCl (13). A rapid decay in absorbance was detected in the region of maximal absorption of the indole group ($\lambda = 280$ nm), the rate of which was linearly dependent on the 3-indolepropionic acid or *N*- α -acetyl-Trp concentrations. This is attributed to direct reaction of 4-imidazoleacetic acid chloramine with the indole ring of the substrate and yielded reproducible second-order rate constants (Table 1). Further absorbance changes were also detected that were fitted by the mechanism shown in eq 1.



The resulting first-order rate constants were, for 3-indolepropionic acid, $k_2 = 0.08 \pm 0.01 \text{ s}^{-1}$ and $k_3 \sim 0.002 \text{ s}^{-1}$ and, for *N*- α -acetyl-Trp, $k_2 = 0.05 \pm 0.02 \text{ s}^{-1}$ and $k_3 \sim 0.008 \text{ s}^{-1}$. These rate constants for the secondary first-order reactions are similar to those determined for HOCl (13), suggesting that common intermediates are produced with both HOCl and 4-imidazoleacetic acid chloramine. The identities of these intermediates and products are not yet known, but one is likely to be the previously detected 2-oxoindole or 2-oxoindolone derivatives (reviewed in ref 10). Formation of a cyclized oxidative cross-link between the Trp side chain and the backbone amide group of -Trp-Gly- motifs has also been reported on oxidation of a matrix metalloproteinase by HOCl (37). While this is a potential product of HOCl-induced Trp oxidation in proteins, it cannot be generated with free or *N*-acetyl-blocked Trp, and therefore, is not responsible for any of the absorbance changes observed in these studies. A full characterization of the oxidation products of isolated Trp and related indolic derivatives will be presented in a future publication.

As the transfer reaction from imidazole chloramines to the Trp side chain is potentially of major significance, due to its high second-order rate constant, the reaction of 3-indolepropionic acid with *N*- α -acetyl-His chloramine was also investigated. Similar kinetic behavior was observed, and the data were analyzed using the mechanism in eq 1. The resulting second-order rate constants are virtually identical for both chloramines (Table 1), and the subsequent first-order rate constants are also very similar; for *N*- α -acetyl-His chloramine, $k_2 = 0.076 \pm 0.002 \text{ s}^{-1}$ and $k_3 \sim 0.005 \text{ s}^{-1}$.

Kinetics of His Side-Chain Chloramine Reactions with the Tyr Side Chain. The rates of chlorination of Tyr residues by imidazole chloramines were studied at 22 °C using the chloramines of both 4-imidazoleacetic acid and *N*- α -acetyl-His and two models for the Tyr side-chain: 3-(4-hydroxyphenyl)propionic acid and *N*- α -acetyl-Tyr. The reactions were studied (over 45 min) with 50 μ M chloramine and 0.3–1.0 mM substrate yielding small absorbance changes ($\Delta A < 0.03$) either side (λ 240–260 nm and λ 290–320 nm) of the main phenol absorption band ($\lambda_{\max} \sim 270$ nm). These changes are characteristic of 3-chlorination or 3,5-dichlorination of these substrates (13). HPLC studies indicated that negligible dichlorination occurs at these concentrations; thus, the data were readily analyzed using a simple mechanism (e.g., 4-imidazoleacetic acid chloramine + 3-(4-hydroxyphenyl)propionic acid \rightarrow 4-imidazoleacetic acid + 3-(3-chloro-4-hydroxyphenyl)propionic acid) to yield consistent second-order rate constants (Table 1) for all four combinations of chloramine and substrate.

Kinetics of His Side-Chain Chloramine Reactions with the Arg Side Chain. Reaction with the guanidine group of the Arg side chain was examined using 4-imidazoleacetic acid chloramine (0.5 mM) and the model compound ethyl guanidine (3.2–10.0 mM) at 22 °C. The absorbance was found to increase at all monitored wavelengths (230–320 nm) over a time scale of 30 min. These changes were accurately fitted using a simple mechanism (4-imidazoleacetic acid chloramine + ethyl guanidine \rightarrow 4-imidazoleacetic acid + product) to yield the second-order rate constant given in Table 1.

HPLC Analysis of *N*- α -acetyl-Tyr Chlorination by Chloramines and Chloramides. As Cl-Tyr is often employed as a marker for HOCl-mediated protein oxidation (26), it is important to understand how this species is generated and whether the level of this product reflects direct oxidation by HOCl and/or chlorination by some or all chloramines. Previous studies have reported that Lys chloramines are capable of chlorinating Tyr and that these species may direct HOCl-mediated damage to such residues in proteins (27). Both experimental and modeling studies have indicated that multiple chlorinating agents are formed on proteins including His and Lys side-chain chloramines, α -amino group chloramines, and backbone chloramides (13, 23, 24). HPLC studies have therefore been undertaken to compare the rate and quantify the extent of *N*- α -acetyl-Tyr chlorination by chloramines/amides under identical conditions. *N*- α -acetyl-Tyr (1.0 mM) was reacted with HOCl, the chloramines of 4-imidazoleacetic acid, *N*- α -acetyl-His (both His side-chain chloramines), ϵ -amino-*n*-caproic acid (a Lys side-chain chloramine model), and Gly (an α -amino chloramine), and the chloramide of *cyclo*-(Gly)₂ (a backbone chloramide model) (all ca. 125 μ M) over a period of 9 days, with samples

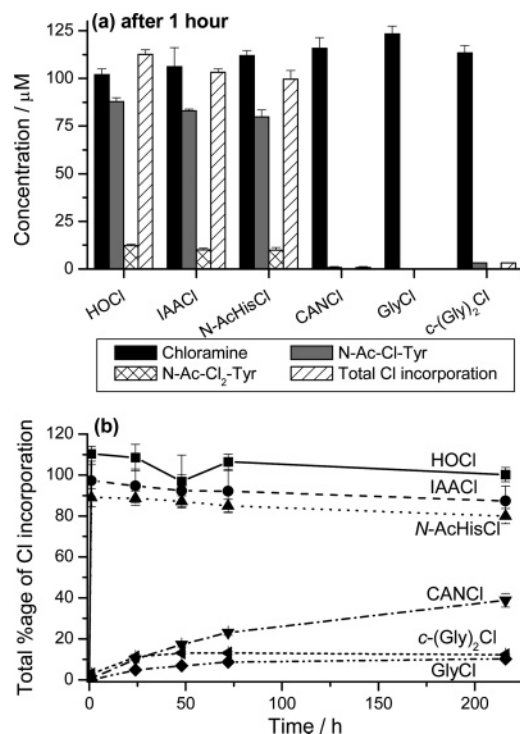


FIGURE 3: Graphs showing the extent of chlorine transfer from HOCl, the imidazole chloramines of 4-imidazoleacetic acid (IAACl) and *N*- α -acetyl-His (*N*-AcHisCl), the chloramines of ϵ -amino-*n*-caproic acid (a Lys side-chain chloramine model; CANCl) and Gly (an α -amino chloramine; GlyCl), and the chloramide of *cyclo*-(Gly)₂ (a backbone chloramide model; *c*-(Gly)₂Cl) to *N*- α -acetyl-Tyr (1.0 mM) as determined by electrochemical detection (+1.2 V). (a) Concentrations detected when the reactions were quenched with *N*- α -acetyl-Cys 1 h after mixing. The concentration (μ M) of chlorinating agent added (determined by the TNB assay) is shown (black column), together with the *N*-Ac-Cl-Tyr (gray column) and *N*-Ac-Cl₂-Tyr (crosshatched column) concentrations detected. The total extent of chlorine incorporation (μ M) into *N*- α -acetyl-Tyr is also shown (hashed columns). (b) A time course showing the total percentage of chlorine incorporation (relative to the chloramine added) into *N*- α -acetyl-Tyr over a period of 9 days. All data are represented as the mean \pm standard deviation ($n = 3$); all data points include error bars, but in some cases, these are smaller than the symbol size.

removed for analysis at 1, 24, 48, and 72 h. Chlorination of *N*- α -acetyl-Tyr was assessed using both UV and electrochemical detection; no significant differences were observed in the values obtained using these two detectors ($p > 0.05$). The extent of chlorine incorporation for *N*-Ac-Cl-Tyr is directly equivalent to its concentration, but for the dichlorinated *N*-Ac-Cl₂-Tyr, the chlorine incorporation is calculated as double its concentration.

HOCl-mediated chlorination of *N*- α -acetyl-Tyr resulted in incorporation of 85% of the available chlorine into *N*-Ac-Cl-Tyr and 20% into *N*-Ac-Cl₂-Tyr within 1 h of mixing (Figure 3a). The imidazole chloramines also chlorinated *N*- α -acetyl-Tyr efficiently (Figure 3a), with 70–80% conversion to *N*-Ac-Cl-Tyr and 15–20% of the active chlorine incorporated into *N*-Ac-Cl₂-Tyr within 1 h. There was a small but significant ($p < 0.01$) decrease in chlorine transfer efficiency by the His side-chain chloramines relative to HOCl, but the differences observed between the two chloramines were insignificant ($p > 0.05$). No further increases in chlorinated *N*- α -acetyl-Tyr levels were detected up to 9 days.

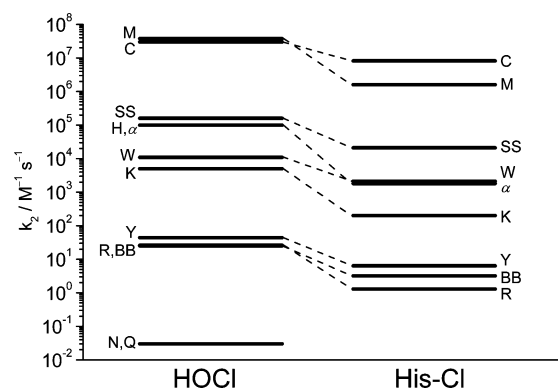


FIGURE 4: Schematic diagram summarizing the second-order rate constants (on a log scale) for the reactions of HOCl (from ref 13) and His chloramine (His-Cl; this paper) with amino acid side chains and other reactive protein components. The value for the backbone amides (BB) represents that determined for *cyclo*-(Gly)₂ and provides a maximal estimate of the rate that occurs in proteins. The following abbreviations are used: M, Met; C, Cys; SS, cystine (disulfide bond); H, His; α , α -amino group (e.g., Gly); W, Trp; K, Lys; Y, Tyr; R, Arg; BB, backbone amide group; N, Asn; Q, Gln.

In contrast to the behavior of the His side-chain chloramines, reaction of *N*- α -acetyl-Tyr with the Lys side-chain chloramine model (ϵ -amino-*n*-caproic acid chloramine) resulted in very low levels of chlorine incorporation (<1%) after 1 h (Figure 3a), with maximal chlorine incorporation of ~40% achieved by 9 days (Figure 3b). At this time point, no chloramine remained as assessed by the TNB assay. The major product was *N*-Ac-Cl-Tyr, with only low yields of *N*-Ac-Cl₂-Tyr detected. Similar behavior was observed for the α -amino chloramine of Gly, with no transfer detected after 1 h (Figure 3a) and only 10% incorporation into *N*-Ac-Cl-Tyr after 9 days (Figure 3b), when the chloramine was fully consumed. No *N*-Ac-Cl₂-Tyr was detected with the chloramine of Gly.

The chloramide of *cyclo*-(Gly)₂ (a model for backbone chloramides), chlorinated *N*- α -acetyl-Tyr more rapidly than the model α -amino or Lys side-chain chloramines, with ~2% incorporation of chlorine into *N*-Ac-Cl-Tyr after 1 h (Figure 3a). Maximal chlorine incorporation of 13% into *N*-Ac-Cl-Tyr was reached within 24–48 h (Figure 3b); no further significant changes in the levels of chlorinated *N*- α -acetyl-Tyr were detected up to 9 days (Figure 3b). No *N*-Ac-Cl₂-Tyr was detected at any time with *cyclo*-(Gly)₂ chloramide as the chlorinating agent.

DISCUSSION

The second-order rate constants obtained for reaction of His side-chain chloramines with protein components are summarized in Figure 4 and compared with those obtained previously for HOCl (13). Typically, the reactivity of the His side-chain chloramine models is only 5–10 times less than that for HOCl, though reaction with the Lys and Arg side-chain models (25-fold) and the α -amino group (50-fold) are noticeably lower. As reported for other chloramines (20, 21), the second-order rate constant for reaction with Met is markedly reduced (25-fold less than for HOCl) compared with that for Cys (a 4-fold decrease), resulting in greater selectivity for thiol depletion over Met sulfoxide formation by chloramines.

The second-order rate constants determined for His side-chain chloramines are among the fastest chlorine transfer processes reported and, as hypothesized, compare well with those for the heterocyclic chloramines (R_2NCl) formed on thymidine and uridine (18, 31). Thus, the rate constants for the reactions of the heterocyclic chloramines of thymidine and uridine with the thiol group of GSH are $\sim 5 \times 10^6 \text{ M}^{-1} \text{ s}^{-1}$ (pH 6.9) (18), in close agreement with the lower limit estimated for the reaction of 4-imidazoleacetic acid chloramine with *N*- α -acetyl-Cys (Table 1). The rate constants for reaction of the heterocyclic chloramines of thymidine and uridine with Gly-Gly-Gly (essentially an α -amino target) are $1.4 \times 10^4 \text{ M}^{-1} \text{ s}^{-1}$ and $5.8 \times 10^3 \text{ M}^{-1} \text{ s}^{-1}$, respectively (pH 6.9) (18), which is slightly faster (5–10-fold) than that reported here for Gly with 4-imidazoleacetic acid chloramine. Similarly, the rates of chlorine transfer from the heterocyclic chloramines of uridine ($26 \text{ M}^{-1} \text{ s}^{-1}$) and thymidine ($22 \text{ M}^{-1} \text{ s}^{-1}$) to the backbone amide model, *cyclo*-(Gly)₂, are slightly faster (ca. 8-fold; (31)) than the corresponding rate constant for 4-imidazoleacetic acid chloramine (Table 1). The high reactivity of these heterocyclic chloramines is due to their ring structure, as the second-order rate constant for the reaction of the exocyclic cytidine chloramine with the thiol group of GSH ($2 \times 10^3 \text{ M}^{-1} \text{ s}^{-1}$) is >2000 -fold slower than the heterocyclic chloramines of thymidine and uridine (18).

The rate constants for other amino acid-derived chloramines, such as those of taurine (Tau), Gly, and *N*- α -acetyl-Lys (20), are much lower than those determined here for His chloramines. Thus, the second-order rate constants for the reactions of Gly chloramine with Met and Cys are ~ 200 and $350 \text{ M}^{-1} \text{ s}^{-1}$, respectively (20), more than 5000 times slower than the rates determined for the His side-chain chloramines. The difference in reactivity between *N*- α -acetyl-Lys and Tau chloramines relative to His chloramines is even more dramatic, with the rate constants for the former pair of compounds more than 2×10^4 times smaller (20). A recent study has shown that chlorine transfer also occurs between chloramines of comparable reactivity; thus, reaction of Gly chloramine with Tau occurs with a rate constant of $0.3 \text{ M}^{-1} \text{ s}^{-1}$, while Tau chloramine reacts with Gly with $k = 0.1 \text{ M}^{-1} \text{ s}^{-1}$ (19); again, these values are $>10^4$ -fold slower than the corresponding rate constants for 4-imidazoleacetic acid chloramine.

There is considerable interest in the reactions of histamine chloramine (21), as this cell-permeable chloramine has potent biological effects (e.g., increased bronchoconstriction relative to histamine (38)). This compound contains two potential sites of chloramine formation: the free amino group and the imidazole ring. Previous kinetic data suggest that (at neutral pH) the imidazole ring should be the major target of reaction with HOCl ($>90\%$) (13), but the second-order rate constants determined for reaction of histamine chloramine(s) with other substrates (e.g., Met, Cys) are more consistent with the presence of a terminal amine chloramine. This may be readily explained by the kinetic data presented here, which suggest that rapid chlorine transfer from an initial chloramine on the imidazole ring to the free amine group should occur either intra- or intermolecularly; this would result in the formation of a terminal amine chloramine. This hypothesis is currently being explored.

A few rate constants have been previously reported for reaction of backbone chloramides with other protein targets.

Thus, reaction of *cyclo*-(Gly)₂ chloramides with Met and the free thiol of GSH occurs with rate constants, k , of $275 \text{ M}^{-1} \text{ s}^{-1}$ and $>5 \times 10^4 \text{ M}^{-1} \text{ s}^{-1}$, respectively; these values are 10^2 – 10^3 times slower than those reported here for 4-imidazoleacetic acid chloramine, but faster than those for Gly and *N*- α -acetyl-Lys chloramines (31).

The HPLC data for chlorine transfer from chloramines to *N*- α -acetyl-Tyr follow the same trend as the direct kinetic data. *N*- α -acetyl-Tyr chlorination was complete within 1 h with HOCl and the imidazole chloramines, reached a maximum with *cyclo*-(Gly)₂ chloramides after 24 h, but was still increasing after 72 h up to maximal chlorination after 9 days with α -amino or model Lys side-chain chloramines. Thus, although the rate constants for Tyr chlorination by α -amino or Lys side-chain chloramines cannot be measured reliably by UV/vis spectroscopy due to the slow nature of these reactions, the relative order of reactivity is consistent with those obtained for Met (20, 31). No chlorination of *N*- α -acetyl-Tyr by Lys side-chain chloramines was detected after 1 h, consistent with previous studies (26, 27), but prolonged exposure resulted in appreciable yields ($\leq 40\%$) in the absence of other agents. It is of interest that of the nonimidazole chloramines, the Lys side-chain chloramines result in the greatest extent of *N*- α -acetyl-Tyr chlorination; this presumably reflects the rate of competing processes (e.g., hydrolysis), which have been shown to be more important (as judged by the yield of aldehydes) for α -amino chloramines than Lys side-chain chloramines (22). The low extent of *N*- α -acetyl-Tyr chlorination by *cyclo*-(Gly)₂ chloramide, despite its comparatively fast induction of chlorination, is almost certainly due to the competitive hydrolytic cleavage of the chloramide (31). The resulting acyclic chloramine would be expected to behave in a manner similar to Gly chloramine, resulting in only low levels of further *N*- α -acetyl-Tyr chlorination.

The current data are consistent with both direct chlorination of the phenol ring of Tyr by HOCl (13, 39), and via intermediary chloramines/amides (26, 27). Domigan et al. first proposed that chlorinated Tyr could be used as a specific marker for MPO- and HOCl-mediated protein oxidation (26). Their studies on small peptides (e.g., Gly-Gly-Tyr-Arg) displayed a time dependent formation of Cl-Tyr over 2 h. HOCl consumption was complete within 2 min, but the Cl-Tyr formation correlated with the rate of decay of peptide chloramine, presumably situated on the terminal amine site; whether this chlorine transfer occurs via an intra- or intermolecular reaction was not established. Recent studies have proposed that highly selective intramolecular chlorination can occur within proteins (27). Thus exposure of HDL to an 80-fold excess of HOCl for 1 h resulted in $>50\%$ chlorination of Tyr¹⁹², with $<6\%$ chlorination at other Tyr residues in apolipoprotein A-I (apo A-I) (27). Further studies demonstrated that the -Tyr-X-X-Lys- motif (where X = a residue that is unreactive with HOCl) is a favorable sequence for Tyr chlorination (27). This was postulated to arise via the presence of an amphipathic helix where the Lys and Tyr residues lie on the same face with the respective α -carbons within 4.5 Å. Formation of a Lys side-chain chloramine was then proposed to result in facile transfer to the Tyr residue. The Tyr¹⁹² residue of apo A-I is present in such a motif. However, two other Tyr residues of apo A-I are also present in -Tyr-X-X-Lys- motifs but are chlorinated to a much lesser

extent than Tyr¹⁹². This has been attributed to reduced solvent and, thus, HOCl, accessibility due to the protein tertiary structure, and/or to the association of this region of the protein with the lipid component of HDL (27). Inspection of the amino acid sequence of apo A-I reveals another potential explanation for this selectivity: Tyr¹⁹² is immediately adjacent to a His residue (LA¹⁹²H¹⁹³AKAT) and is the only Tyr residue in apo A-I in such proximity to a His residue. As kinetic studies suggest that His residues are a major target of HOCl (13) and the resulting His side-chain chloramines have been demonstrated here to undergo rapid chlorine transfer with Tyr residues (Table 1, Figure 3), it is possible that the targeted chlorination of Tyr¹⁹² in apo A-I (27) arises via the intermediacy of His, rather than Lys, chloramines; this is currently being tested.

Nightingale et al. have reported previously that reaction of HOCl with a 1:1 mixture of *N*- α -acetyl-Gly-Glu-His-Phe and *N*- α -acetyl-Ala-Glu-Lys-Phe resulted only in the detection of mono- and dichlorinated *N*- α -acetyl-Ala-Glu-Lys-Phe (40). This is initially surprising given the previously reported rate constants for reaction of HOCl with His and Lys residues (13), but is readily explicable by the rate constants determined here, as rapid chlorine transfer would be expected to occur from the His residue to the Lys site.

In summary, the kinetic data obtained in this work highlight the importance of chloramine structure on their subsequent reactivity and show that His side-chain chloramines are important intermediates in HOCl-mediated protein oxidation. In particular, His residues are not only major sites of initial HOCl attack, but important secondary oxidants of other residues, due to the high reactivity of the resulting side-chain chloramines. This could result in much higher levels of oxidation of some residues (e.g., cystine, Trp, Tyr, and Lys) than might initially be expected. A further implication of this work is that chlorination of His residues may provide a conduit for the targeted oxidation of selected residues in proteins (e.g., as observed for Tyr¹⁹² in apo A-I (27)), whether these be close in sequence, or spatially. These chlorine transfer reactions of His side-chain chloramines would also be predicted to occur intermolecularly and may result in the induction of secondary damage both to other proteins and potentially other biological targets such as DNA and lipids. Further work is required to elucidate the full extent and biological significance of these reactions.

ACKNOWLEDGMENT

The authors thank Prof. Peter Lay and Dr. Aviva Levina (University of Sydney), for the use of the Applied Photophysics SX.18MV stopped flow system, and Dr. Clare Hawkins (The Heart Research Institute), for helpful discussions.

REFERENCES

- Zgliczynski, J. M., Stelmaszynska, T., Ostrowski, W., Naskalski, J., and Sznajd, J. (1968) Myeloperoxidase of human leukaemic leucocytes. Oxidation of amino acids in the presence of hydrogen peroxide, *Eur. J. Biochem.* 4, 540–547.
- Morris, J. C. (1967) Kinetics of reactions between aqueous chlorine and nitrogen compounds, in *Principles and Applications of Water Chemistry* (Faust, E. D., and Hunter, J. V., Eds.) pp 23–53, John Wiley and Sons, New York.
- Klebanoff, S. J. (1999) Myeloperoxidase, *Proc. Assoc. Am. Physicians* 111, 383–389.
- Hoy, A., Leininger-Muller, B., Kutter, D., Siest, G., and Visvikis, S. (2002) Growing significance of myeloperoxidase in non-infectious diseases, *Clin. Chem. Lab. Med.* 40, 2–8.
- Malle, E., Buch, T., and Grone, H.-J. (2003) Myeloperoxidase in kidney disease, *Kidney Int.* 64, 1956–1967.
- Podrez, E. A., Abu-Soud, H. M., and Hazen, S. L. (2000) Myeloperoxidase-generated oxidants and atherosclerosis, *Free Radical Biol. Med.* 28, 1717–1725.
- Zhang, R., Brennan, M. L., Fu, X., Aviles, R. J., Pearce, G. L., Penn, M. S., Topol, E. J., Sprecher, D. L., and Hazen, S. L. (2001) Association between myeloperoxidase levels and risk of coronary artery disease, *J. Am. Med. Assoc.* 286, 2136–2142.
- Weitzman, S. A., and Gordon, L. I. (1990) Inflammation and cancer: role of phagocyte-generated oxidants in carcinogenesis, *Blood* 76, 655–663.
- van der Vliet, A., Nguyen, M. N., Shigenaga, M. K., Eiserich, J. P., Marelich, G. P., and Cross, C. E. (2000) Myeloperoxidase and protein oxidation in cystic fibrosis, *Am. J. Physiol. Lung Cell. Mol. Physiol.* 279, L537–L546.
- Hawkins, C. L., Pattison, D. I., and Davies, M. J. (2003) Hypochlorite-induced oxidation of amino acids, peptides and proteins, *Amino Acids* 25, 259–274.
- Armesto, X. L., Canle, M., Garcia, M. V., and Santaballa, J. A. (1998) Aqueous chemistry of *N*-halo-compounds, *Chem. Soc. Rev.* 27, 453–460.
- Winterbourn, C. C. (1985) Comparative reactivities of various biological compounds with myeloperoxidase-hydrogen peroxide-chloride, and similarity of the oxidant to hypochlorite, *Biochim. Biophys. Acta* 840, 204–210.
- Pattison, D. I., and Davies, M. J. (2001) Absolute rate constants for the reaction of hypochlorous acid with protein side-chains and peptide bonds, *Chem. Res. Toxicol.* 14, 1453–1464.
- Armesto, X. L., Canle, M., Fernandez, M. I., Garcia, M. V., and Santaballa, J. A. (2000) First steps in the oxidation of sulfur-containing amino acids by hypohalogenation: very fast generation of intermediate sulfonyl halides and halosulfonium cations, *Tetrahedron* 56, 1103–1109.
- Folkes, L. K., Candeias, L. P., and Wardman, P. (1995) Kinetics and mechanisms of hypochlorous acid reactions, *Arch. Biochem. Biophys.* 323, 120–126.
- Thomas, E. L., Grisham, M. B., and Jefferson, M. M. (1986) Preparation and characterization of chloramines, *Methods Enzymol.* 132, 569–585.
- Prutz, W. A. (1998) Reactions of hypochlorous acid with biological substrates are activated catalytically by tertiary amines, *Arch. Biochem. Biophys.* 357, 265–273.
- Prutz, W. A. (1998) Interactions of hypochlorous acid with pyrimidine nucleotides, and secondary reactions of chlorinated pyrimidines with GSH, NADH, and other substrates, *Arch. Biochem. Biophys.* 349, 183–191.
- Peskin, A. V., Midwinter, R. G., Harwood, D. T., and Winterbourn, C. C. (2004) Chlorine transfer between glycine, taurine and histamine: reaction rates and impact on cellular reactivity, *Free Radical Biol. Med.* 37, 1622–1630.
- Peskin, A. V., and Winterbourn, C. C. (2001) Kinetics of the reactions of hypochlorous acid and amino acid chloramines with thiols, methionine, and ascorbate, *Free Radical Biol. Med.* 30, 572–579.
- Peskin, A. V., and Winterbourn, C. C. (2003) Histamine chloramine reactivity with thiol compounds, ascorbate, and methionine and with intracellular glutathione, *Free Radical Biol. Med.* 35, 1252–1260.
- Hazen, S. L., d'Avignon, A., Anderson, M. A., Hsu, F. F., and Heinecke, J. W. (1998) Human neutrophils employ the myeloperoxidase-hydrogen peroxide-chloride system to oxidize α -amino acids to a family of reactive aldehydes, *J. Biol. Chem.* 273, 4997–5005.
- Hawkins, C. L., and Davies, M. J. (1998) Reaction of HOCl with amino acids and peptides: EPR evidence for rapid rearrangement and fragmentation reactions of nitrogen-centered radicals, *J. Chem. Soc., Perkin Trans. 2*, 1937–1945.
- Hawkins, C. L., and Davies, M. J. (1998) Hypochlorite-induced damage to proteins: formation of nitrogen-centred radicals from lysine residues and their role in protein fragmentation, *Biochem. J.* 332, 617–625.
- Hawkins, C. L., Rees, M. D., and Davies, M. J. (2002) Superoxide radicals can act synergistically with hypochlorite to induce damage to proteins, *FEBS Lett.* 510, 41–44.

26. Domigan, N. M., Charlton, T. S., Duncan, M. W., Winterbourn, C. C., and Kettle, A. J. (1995) Chlorination of tyrosyl residues in peptides by myeloperoxidase and human neutrophils, *J. Biol. Chem.* 270, 16542–16548.
27. Bergt, C., Fu, X., Huq, N. P., Kao, J., and Heinecke, J. W. (2004) Lysine residues direct the chlorination of tyrosines in YXXK motifs of apolipoprotein A-I when hypochlorous acid oxidizes HDL, *J. Biol. Chem.* 279, 7856–7866.
28. Hsu, Y.-C. (1964) Resistance of infectious RNA and transforming DNA to iodine which inactivates f2 phage and cells, *Nature* 203, 152–153.
29. Vissers, M. C. M., Lee, W. G., and Hampton, M. B. (2001) Regulation of apoptosis by vitamin C: specific protection of the apoptotic machinery against exposure to chlorinated oxidants, *J. Biol. Chem.* 276, 46835–46840.
30. Thomas, E. L., Grisham, M. B., and Jefferson, M. M. (1986) Cytotoxicity of chloramines, *Methods Enzymol.* 132, 585–593.
31. Prutz, W. A. (1999) Consecutive halogen transfer between various functional groups induced by reaction of hypohalous acids: NADH oxidation by halogenated amide groups, *Arch. Biochem. Biophys.* 371, 107–114.
32. Pattison, D. I., Hawkins, C. L., and Davies, M. J. (2003) Hypochlorous acid mediated oxidation of lipid components and antioxidants present in low density lipoproteins: absolute rate constants, product analysis and computational modeling, *Chem. Res. Toxicol.* 16, 439–449.
33. Morris, J. C. (1966) The acid ionization constant of HOCl from 5 °C to 35 °C, *J. Phys. Chem.* 70, 3798–3805.
34. Pattison, D. I., and Davies, M. J. (2004) Kinetic analysis of the reactions of hypobromous acid with protein components: implications for cellular damage and use of 3-bromotyrosine as a marker of oxidative stress, *Biochemistry* 43, 4799–4809.
35. Hunt, S. (1984) Halogenated tyrosine derivatives in invertebrate scleroproteins: isolation and identification, *Methods Enzymol.* 107, 413–438.
36. Prutz, W. A., Kissner, R., Koppenol, W. H., and Ruegger, H. (2000) On the irreversible destruction of reduced nicotinamide nucleotides by hypohalous acids, *Arch. Biochem. Biophys.* 380, 181–191.
37. Fu, X., Kao, J. L. F., Bergt, C., Kassim, S. Y., Huq, N. P., d'Avignon, A., Parks, W. C., Mecham, R. P., and Heinecke, J. W. (2004) Oxidative cross-linking of tryptophan to glycine restrains matrix metalloproteinase activity: specific structural motifs control protein oxidation, *J. Biol. Chem.* 279, 6209–6212.
38. Wright, C. D., and Low, J. E. (1989) Formation of chloramine derivatives of histamine: role of histamine chloramines in bronchoconstriction, *Biochem. Biophys. Res. Commun.* 165, 1018–1026.
39. Fu, S., Wang, H., Davies, M. J., and Dean, R. T. (2000) Reaction of hypochlorous acid with tyrosine and peptidyl-tyrosyl residues gives dichlorinated and aldehydic products in addition to 3-chloro-tyrosine, *J. Biol. Chem.* 275, 10851–10857.
40. Nightingale, Z. D., Lancha, A. H., Jr., Handelman, S. K., Dolnikowski, G. G., Busse, S. C., Dratz, E. A., Blumberg, J. B., and Handelman, G. J. (2000) Relative reactivity of lysine and other peptide-bound amino acids to oxidation by hypochlorite, *Free Radical Biol. Med.* 29, 425–433.

BI0474665